Solar Energy Materials & Solar Cells 95 (2011) 699–703

Contents lists available at ScienceDirect

Solar Energy Materials & Solar Cells

journal homepage: www.elsevier.com/locate/solmat

2-Step self-assembly method to fabricate broadband omnidirectional antireflection coating in large scale

K.M. Yeung [a], W.C. Luk [a], K.C. Tam [a], C.Y. Kwong [a,*], M.A. Tsai [b], H.C. Kuo [b], A.M.C. Ng [c], A.B. Djurišić [c]

[a] Nano and Advanced Materials Institute Ltd., Unit 608–609, Lakeside 2, Hong Kong Science Park, Shatin, HK, China
[b] Institute of Electro-Optical Engineering, National Chiao Tung University, Hsinchu 300, Taiwan, ROC
[c] Department of Physics, The University of Hong Kong, Pokfulam Road, HK, China

ARTICLE INFO

Article history:
Received 3 August 2010
Accepted 4 October 2010
Available online 20 October 2010

Keywords:
Nano silica
Antireflection
Self-assembly
Broadband
Omnidirectional

ABSTRACT

We have developed a simple and reproducible 2-step self-assembly method for the fabrication of broadband, omnidirectional antireflection coating on glass substrate with 4 in. size. The glass surface has been modified to be positively charged, then the negatively charged nano silica is self-assembled to the glass substrate by electrostatic attraction. The nanostructure on the glass substrate reduces the reflection significantly, which results in enhanced transmittance. Transmittance as high as 97.7% at 499 nm has been obtained for a double-side coated glass substrate. Obvious reduction in weighted reflectance is still observed up to 60° incident angle.

1. Introduction

Photovoltaic technology has been getting more importance nowadays due to the increased demand in the green energy [1,2]. To improve its efficiency, antireflection coating is an essential component in any kind of photovoltaic cells. The common antireflection coating used in silicon solar cell is a single layer homogenous SiN_x deposited by an expensive PECVD process. The SiN_x single layer is simple, but there are two major drawbacks in addition to the cost. A single layer SiN_x can only be optimized for minimum reflection at a particular wavelength of interests, the reflectance increases when the wavelength is offset from the target value. Broadband low reflectance can be achieved with multilayer antireflection coating consisting of high and low refractive index materials, but this increases the complexity. The reflectance also increases sharply with increase in incident angles for homogeneous thin films. This would result in a reduction of conversion efficiency for oblique incidence of the sunlight, which would be a significant disadvantage.

Therefore, there have been considerable efforts in developing a broadband, omnidirectional antireflection coating in an effective and simple way [3–13]. Oblique angle electron beam deposition is one of the methods to fabricate broadband omnidirectional antireflection coating [14,15]. Using this method, a porous nanostructured thin film can be obtained. This allows us to control the refractive index of the material by controlling the porosity. Chhajed et al. [14] have investigated the use of oblique angle electron beam deposition for antireflection coating. The trilayer structure they used is bulk TiO_2 ($n=2.66$)/bulk SiO_2 ($n=1.47$)/porous TiO_2 (80% porosity, $n=1.07$) [14]. The refractive index of porous TiO_2 thin film is very close to unity due to its high porosity. The final average reflectance has been reduced to 5.9% compared to 17.3% of the conventional single layer Si_3N_4 antireflection coating [14]. Reflectance was still below 25% at an incident angle of 80° [14]. The low reflectance was attributed to the gradient refractive index of the trilayer structure. Chang et al. [15] have also used the same method to fabricate single layer tapered ITO nanocolumn on silicon substrate. The low reflectance of 6% has been maintained up to 70° incident angle. They have used rigorous coupling wave analysis (RCWA) to calculate the refractive index, and found that the tapered ITO nanocolumn functioned as a gradient refractive index layer. This results in a large reduction in the reflectance. Although this method is promising, the machine geometry is quite complex and the fabrication method is quite expensive.

Compared to vacuum deposition techniques, solution processing, such as self-assembly method or spin coating, represents a simpler and more cost effective thin film fabrication method [17–21]. Jiang and McFarlund [17] and Sun et al. [18] have blended nano silica into a monomer and optimized the spin-coating process and UV curing process to form a regular non-close pack structure on a 4 in. size wafer. Then, a 2-step reactive ion etching (RIE) process was carried out to etch away the polymer and then etch the pattern into the silicon wafer. The nanostructure on the silicon wafer reduces the

* Corresponding author. Tel.: +85235113402; fax: +85222105014.
E-mail addresses: cykwong@gmail.com, cykwong@nami.org.hk (C.Y. Kwong).

0927-0248/$ - see front matter © 2010 Elsevier B.V. All rights reserved.
doi:10.1016/j.solmat.2010.10.005

reflectance dramatically to below 1%. Still, the fabrication steps are a bit complex, involving optimizing a lot of parameters. Self-assembly method, on the other hand, is much simpler. The most critical parameters are the solution concentration and the immersing time only. Zhang et al. [21] have reported using the self-assembly method to assemble multilayers of polycations and polyanions on top of a glass substrate. Glass substrates were first treated by Piranha-solution. The glass surfaces were hydroxylated [22]. Then fabrication was started by self-assembling a polycations, poly diallyldimethylammonium (PDDA), on the glass substrates. Then the polyanion layer, sodium poly(4-styrene sulfonate) (PSS), was self-assembled. These steps were repeated to fabricate four to five PDDA/PSS bilayers. Then, a single layer of PDDA was self-assembled on top of (PDDA/PSS) multilayers to make the surface positively charged. Finally, the negatively charged nano silica and postively charged titanium dioxide were sequentially self-assembled on top of the polymer multilayers by electrostatic attraction [21]. They have successfully demonstrated that the transmittance of the glass was improved as well as keeping the self-cleaning property [21]. The self-cleaning property was demonstrated by the small water contact angle with the TiO_2 nanoparticle coating under UV-A irradiation [21]. However, it is still very time consuming to coat 4–5 bilayers of polycations and polyanions to modify the surface properties of the substrate before coating the nanoparticles.

In this work, our objective is to use a simple and reproducible method to fabricate a broadband and omnidirectional antireflection coating. Compared to the vacuum E-beam techniques [14,15] and the 10–12 self-assembled layers reported by Zhang et al. [21], we attempt to use a simplified self-assembly method to fabricate negatively charged nano silica on glass substrates, which involves only two self-assembled layers and still offer good antireflection property.

2. Experimental details

All the solvents and chemicals are used as received. 3-Aminopropyltrimethyoxysilane (APTMS) was purchased from Lancaster Synthesis Inc. Mono-dispersed nano silica colloidals (MP1040 and MP2040) were supplied by Nissan Kagaku, Japan. The antireflection coatings were prepared on soda lime glasses by self-assembly method on both sides of the glasses. Silicon wafers with native oxide were used instead of glass substrates for surface morphology characterization. The self-assembly method was simple in which no vacuum equipment were needed. Moreover, the method we developed involved only two self-assembled layers. First, all the substrates were thoroughly cleaned before coating the nano silica. Soda lime glass substrates were cleaned with a concentrated H_2SO_4/H_2O_2 (7:3 v/v) solution and then washed with 18 MΩ deionized water, while the silicon substrates were ultrasonicated in ethanol, acetone and deionized water sequentially. The cleaned substrates were then ultrasonicated in methanol, methanol/toluene (1:1) and toluene in sequence. The substrates were then treated by immersing in 1% v/v APTMS in anhydrous toluene solution for 30 min. Then they were briefly rinsed with toluene and immersed in a heat toluene around 80 °C for another 30 min. The cooled substrates were then rinsed and ultrasonicated with methanol/toluene (1:1), methanol and deionized water in a sequence for 2 min each step. The treatment procedure is described in Ref. [23]. By treating with APTMS, the glasses were silanized [22,24]. After rinsing with deionized wafer, the glasses were blow dried by N_2. They were then immersed vertically into the negatively charged mono-dispersed nano silica colloidal solution MP1040, or MP2040 for 5 min, rinsed with deionized water twice and blow dried by N_2. The size of nano silica in MP1040 is around 126 and that of MP2040 is around 200 nm.

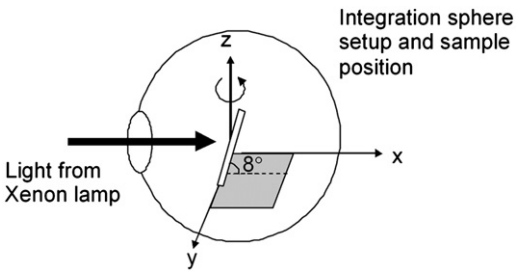

Fig. 1. Schematic diagram of the reflectance measurement system. The sample is placed in the center of the integrated sphere with 8° tilting with the *x*–*y* plane. The sample is rotated through 0–60° for angular dependent reflectance measurement.

Surface morphologies and cross-sections of the antireflection coatings were examined with scanning electron microscopes (JEOL JSM-7001F). The direct transmittances were measured by the Varian Cary 50 UV/Vis Spectrometer. Total transmittances were measured with an integration sphere and a spectrometer with a halogen light source. Reflectances were measured with an integrated sphere, a Xenon lamp and a spectrometer. The samples were placed in the center of the integrated sphere tilted at 8° with the *x*–*y* plane. For angular dependent reflectance measurement, the samples were kept at 8° tilting with the *x*–*y* plane and they were rotated from 0° to 60° about the *z*-axis (Fig. 1). The back side of the sample was covered by a non-reflective black card during the reflectance measurements to avoid unwanted signal transmission through the sample.

3. Results and discussion

Fig. 2 shows the SEM images of the Si wafer coated with MP1040 and MP2040. Since the surface properties of Si wafer with native oxide are similar to those of glass, the morphologies of the samples fabricated on glass substrates are similar to that on Si wafer, which are not shown. The nano silica spheres are self-assembled in a random non-close packed manner for both samples, which is similar to that obtained from Ref. [21]. We have repeated the fabrication process of the MP1040 sample on a 4 in. silicon wafer. Very similar morphology has been obtained at the four corners and at the center of the wafer (SEM images are not shown). The good uniformity and good reproducibility over large area are essential to bring this technology to real applications.

Fig. 3 shows the direct transmittance of soda lime glasses with or without double-side coating of MP1040 or MP2040. The direct transmittance is enhanced in the whole spectrum for MP1040 sample compared to that of the bare glass. The peak transmittance of 97.7% is obtained at 499 nm for the MP1040 sample. The high transmittance and the peak location agree well with a previous report on self-assembly method for antireflective coatings [21]. We have also attempted to tune the transmittance peak by using larger nano sphere MP2040. The coverage of the MP2040 nano silica is about 45%, which results in an effective refractive index equal to 1.25 by the effective medium theory [25,26]. For the MP2040 sample, the transmittance is enhanced from 600 to 900 nm compared to that of the bare glass and the broadband high transmittance of 95.5% from 750 to 900 nm has been observed. For wavelengths shorter than 600 nm, the transmittance of the MP2040 sample is lower than that of the bare glass. Similar observations were reported by coating nano silica with different sizes on glass substrates [27–29]. Yancey et al. [27] investigated coating of nano silica of sizes from 15 to 85 nm . The transmittance was tuned by their film thickness. They also observed the lower transmittance compared to a bare glass for a thicker film. The decrease in peak transmittance was explained by stronger diffuse

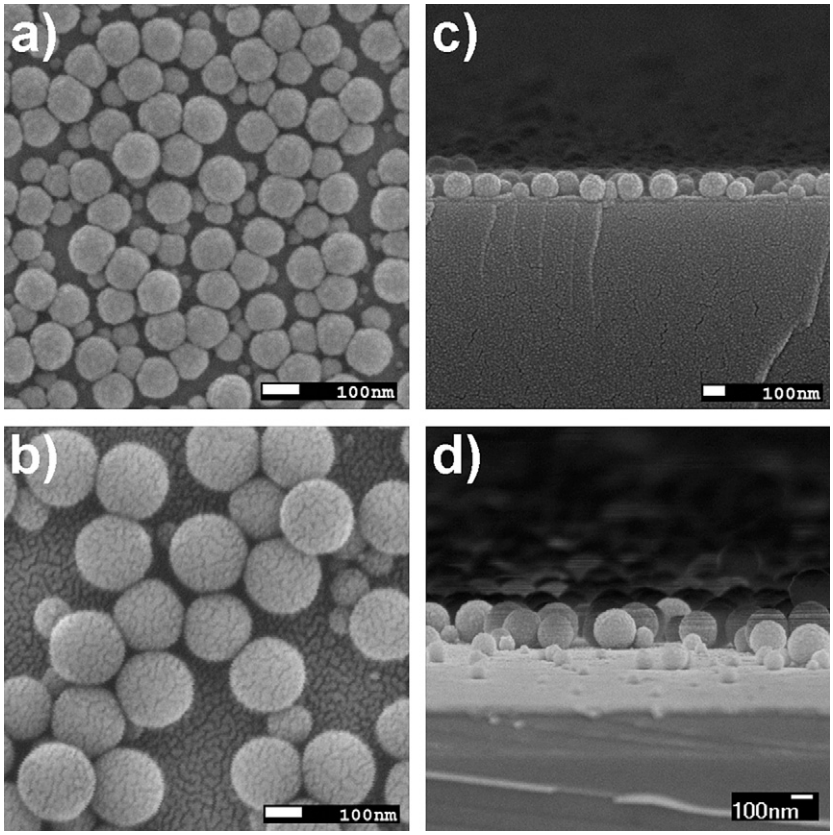

Fig. 2. SEM images of the morphology of (a) MP1040 sample and (b) MP2040 sample; and the cross-sectional images of (c) MP1040 sample and (d) MP2040 sample.

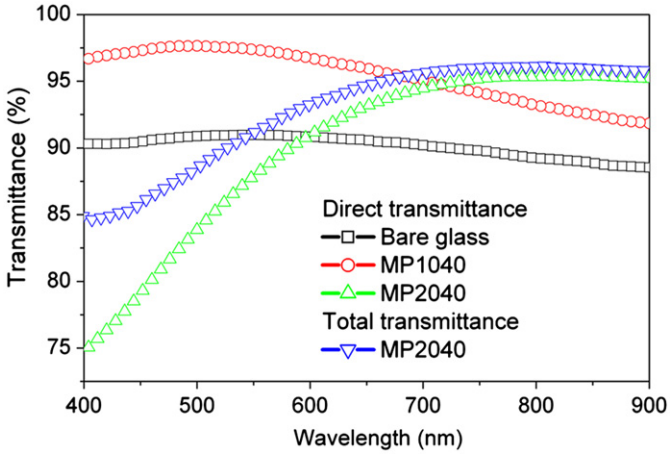

Fig. 3. Direct transmission spectra of MP1040 sample, MP2040 sample and the bare glass. The blue inverted triangle line shows the total transmittance measured with an integration sphere for MP2040 sample. The different in total transmittance and the direct transmittance shows stronger scattering of MP2040 sample in short wavelength region. (For interpretation of the references to color in this figure legend, the reader is referred to the web version of this article.)

scattering, which increases with particle size [27]. Deák et al. [28] also have reported a lower transmittance at wavelengths shorter than ~600 nm compared to bare glass, when two layers of 107 nm silica were coated on a glass substrate . This observation is very similar to our results for a mono-layer of 200 nm silica particles. They explained their results by enhanced absorption in the glass substrate. In our case, the fall in the transmittance in MP2040 sample below the bare glass in our study could be attributed to the enhancement in absorption and in total reflectance. With a single layer antireflection coating of nano silica spheres with 200 nm diameter, the minimum reflectance should occur at ~800 nm. When the wavelength is offset from 800 nm, the reflectance increases. Also, with the 200 nm nano silica sphere, the light scattering property becomes more significant [27]. The larger scattering could increase the haze, which will be useful to improve light trapping efficiency in thin film solar cell applications in addition to the antireflection properties. No obvious scattering is observed in the MP1040 sample. Since the MP1040 sample has overall higher transmittance, we have further characterized it with reflectance measurements.

It can be seen from Fig. 4a that the reflectance of the MP1040 sample is much lower than that of the bare glass in the whole spectrum from 400 to 900 nm, especially in the visible region. The minimum reflectance occurs at around 435 nm. The reduction in the reflectance might be attributed to the lower effective refractive index of the coating, which is about 1.38 calculated by the effective medium theory with 74.5% coverage of nano silica. The optical thickness for minimum reflection occurring at 435 nm should be equal to $\lambda/4$ (~109 nm). This value is consistent with the diameter of the nano silica (~126 ± 13 nm). For the MP2040 sample, the reflectance minimum should be around 800 nm (4 times the diameter of the MP2040 particle), which is also in good agreement with the high transmittance observed in Fig. 3. By using particles with different sizes or by fabricating antireflection coating with different thicknesses, the transmittance and the reflectance can be controlled.

Fig. 4b shows the weighted reflectance at different incident angles calculated according to the following equation:

$$R_w = \int_{400}^{900} R(\lambda)I(\lambda)d\lambda / \int_{400}^{900} I(\lambda)d\lambda \quad (1)$$

where R_w is the weighted reflectance, R is the reflectance from 400 to 900 nm, and $I(\lambda)$ is the intensity of light at particular wavelength

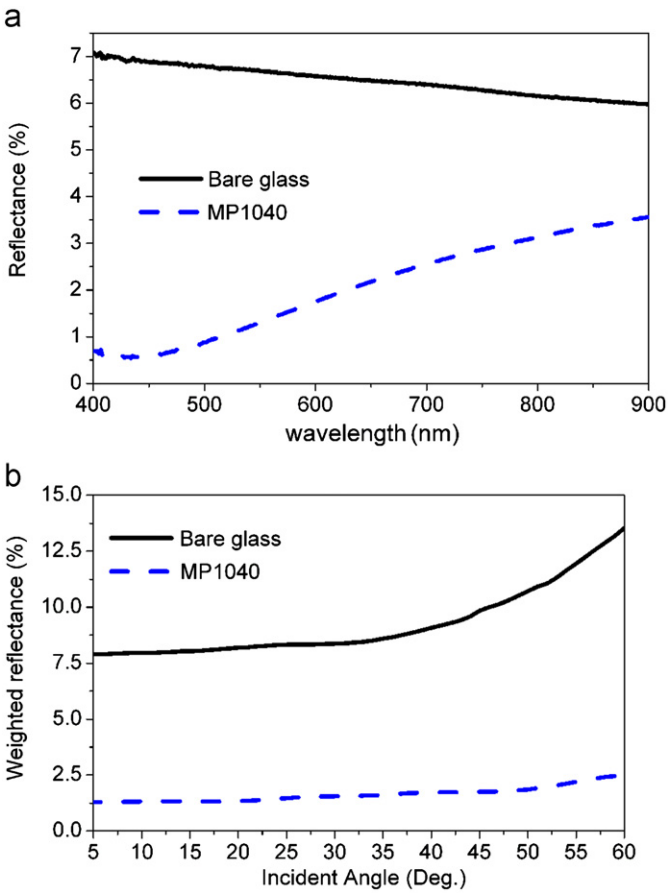

Fig. 4. (a) Reflectance measurement at 8° incident angle and (b) weighted reflectance at different incident angles.

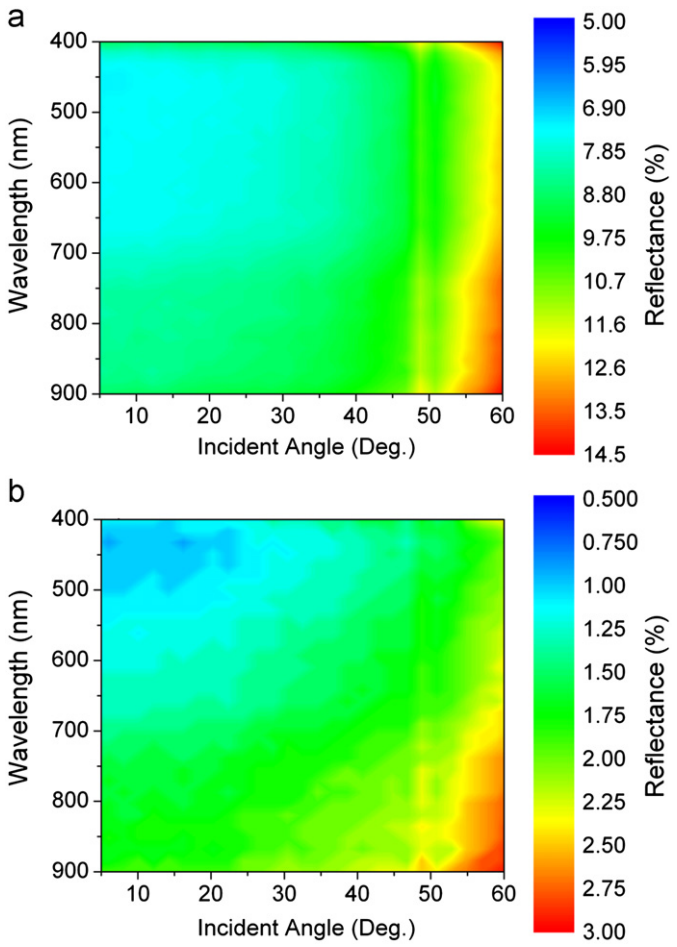

Fig. 5. Angular dependent reflectance of (a) bare glass and (b) MP1040 sample.

and measured $R(\lambda)$ is the reflectance at a particular wavelength. The weighted reflectance is still much lower than the bare glass even at a large incident angle of 60°. Also, at large incident angles, where the glass weighted reflectance increases sharply, the reflectance of MP1040 sample only slightly increases.

Fig. 5a and b shows the angular dependent reflectance of bare glass and MP1040 sample, respectively. The reflectance of the MP1040 sample has been suppressed significantly from 400 to 900 nm even at a large incident angle of 60° compared to that of the bare glass. At this angle, the reflectance at longer wavelengths starts to increase, but it is still well below 3.5%, while the reflectance of glass is above 12% in the whole spectrum at 60° incident angle. The broadband low reflectance with omnidirectional properties might be attributed to both the lower effective refractive index, the graded-index profile and the spherical shape of the silica [8,10–16]. The reduction in reflectance can result in enhancement in the power conversion efficiency of a solar cell [30,31]. More importantly, the low reflectance at larger incident angle can minimize the variation of power conversion efficiency in a day. Thus, a simpler solar system can be designed.

4. Conclusion

In summary, broadband omnidirectional antireflection coating has been fabricated by a simple 2-step self-assembly method on a 4 in. substrate. The reflectance of the MP1040 sample has been reduced significantly to less than 3% in the whole spectrum from 400 to 900 nm. This results in ultrahigh transmittance of 97.7% at 499 nm for a soda lime glass with MP1040 coated on both sides. The weighted reflectance of the MP1040 sample is much lower than the bare glass and well below 3% at 60° incident angle. In this method, the optical properties can be tuned by using nano spheres of different sizes, or different thicknesses of antireflection coating. We have demonstrated that the transmittance peak can be shifted by using a larger nano silica (MP2040 ~200 nm) to ~800 nm. The fabrication method also shows a good uniformity and reproducibility for a 4 in. substrate. We believe that a simple, reproducibleand low cost method to fabricate broadband omnidirectional antireflection coating should have a large impact in photovoltaic applications.

Acknowledgement

This work has been supported by HKSAR Innovation and Technology Fund (ITP/030/09NP).

References

[1] C.Y. Kwong, W.C.H. Choi, A.B. Djurišić, P.C. Chui, K.W. Cheng, W.K. Chan, Poly(3-hexylthiophene):TiO_2 nanocomposites for solar cell applications, Nanotechnology 15 (2004) 1156–1161.
[2] C.Y. Kwong, A.B. Djurišić, P.C. Chui, K.W. Cheng, W.K. Chan, Influence of solvent on film morphology and device performance of poly(3-hexylthiophene):TiO_2 nanocomposite solar cells, Chem. Phys. Lett. 384 (2004) 372–375.
[3] J. Zhu, Z. Yi, G.F. Burkhard, C.M. Hsu, S.T. Connor, Y. Xu, Q. Wang, M. McGehee, S. Fan, Y. Cui, Optical absorption enhancement in amorphous silicon nanowire and nanocone arrays, Nano Lett. 9 (2008) 279–282.
[4] C.M. Hsu, S.T. Connor, M.X. Tang, Y. Chi, Wafer-scale silicon nanopillars and nanocones by Langmuir–Blodgett assembly and etching, Appl. Phys. Lett. 91 (2008) 133109-1–133109-3.

[5] P. Jiang, T. Prasad, M.J. McFarland, V.L. Covin, Two-dimensional nonclose-packed colloidal crystals formed by spincoating, Appl. Phys. Lett. 89 (2006) 011908-1–011908-3.
[6] Y. Wang, L. Chen, H. Yang, Q. Guo, W. Zhou, M. Tao, Spherical antireflection coatings by large-scale convective assembly of monolayer silica microspheres, Sol. Energy Mater. Sol. Cells 93 (2009) 85–91.
[7] M. Manca, A. Cannavale, L.D. Marco, A. Aricò, R. Cingolani, G. Gigli, Durable superhydrophobic and antireflective surfaces by trimethysilanized silica nanoparticles-based sol–gel processing, Langmuir 25 (2009) 6357–6362.
[8] C.C. Chen, D.J. Lin, T.M. Don, F.H. Huang, L.P. Cheng, Preparation of organic–inorganic nano-composites for antireflection coatings, J. Non-Cryst. Solids 354 (2008) 3828–3835.
[9] Q. Chen, G. Hubbard, P.A. Shields, C. Liu, D.W.E. Allsopp, W.N. Wang, S. Abbott, Broadband moth-eye antireflection coatings fabricated by low-cost nanoimprinting, Appl. Phys. Lett. 94 (2009) 263118-1–263118-3.
[10] D.J. Poxson, M.F. Schubert, F.W. Mont, E.F. Schubert, J.K. Kim, Broadband omnidirectional antireflection coatings optimized by genetic algorithm, Opt. Lett. 34 (2009) 728–730.
[11] S.L. Diedenhofen, G. Vecchi, R.E. Algra, A. Hartsuiker, O.L. Muskens, G. Immink, E.P.A.M. Bakkers, W.L. Vos, J.G. Rivas, Broad-band and omnidirectional antireflection coatings based on semiconductor nanorods, Adv. Mater. 21 (2008) 973–978.
[12] B.J. Bae, S.H. Hong, E.J. Hong, H. Lee, G.Y. Jung, Fabrication of moth-eye structure on glass by ultraviolet imprinting process with polymer template, Jpn. J. Appl. Phys. 48 (2009) 010207-1–010207-3.
[13] M.J. Kuo, D.J. Poxson, Y.S. Kim, F.W. Mont, J.K. Kim, E.F. Schubert, S.Y. Lin, Realization of a near-perfect antireflection coating for silicon solar energy utilization, Opt. Lett. 33 (2008) 2527–2529.
[14] S. Chhajed, M.F. Schubert, J.K. Kim, E.F. Schubert, Nanostructured multilayer graded-index antireflection coating for Si solar cells with broadband and omnidirectional characteristics, Appl. Phys. Lett. 93 (2008) 251108-1–251108-3.
[15] C.H. Chang, P. Yu, C.S. Yang, Broadband and omnidirectional antireflection from conductive indium-tin-oxide nanocolumns prepared by glancing-angle deposition with nitrogen, Appl. Phys. Lett. 94 (2009) 051114-1–051114-3.
[16] W.L. Min, P. Jiang, B. Jiang, Large-scale assembly of colloidal nanoparticles and fabrication of periodic subwavelength structures, Nanotechnology 19 (2008) 475604 (7pp).
[17] P. Jiang, M.J. McFarland, Large-scale fabrication of wafer-size colloidal crystals, macroporous polymers and nanocomposites by spin-coating, J. Am. Chem. Soc. 126 (2004) 13778–13786.
[18] C.H. Sun, W.L. Min, N.C. Linn, P. Jiang, Large-scale assembly of periodic nanostructures with metastable square lattices, J. Vac. Sci. Technol. B 27 (2009) 1043–1047.
[19] T. Soeno, K. Inokuchi, S. Shiratori, Ultra-water-repellent surface: fabrication of complicated structure of SiO_2 nanoparticles by electrostatic self-assembled films, Appl. Surf. Sci. 237 (2004) 543–547.
[20] H. Hattori, Anti-reflection surface with particle coating deposited by electrostatic attraction, Adv. Mater. 13 (2001) 51–54.
[21] X.T. Zhang, O. Sato, M. Taguchi, Y. Einaga, T. Murakami, A. Fujishima, Self-cleaning particle coating with antireflection properties, Chem. Mater. 17 (2005) 696–700.
[22] G. Arslan, M. Özmen, B. Gündüz, X. Zhang, M. Ersöz, Surface modification of glass beads with aminosilane monolayer, Turk. J. Chem. 30 (2006) 203–210.
[23] C.W. Tse, K.Y.K. Man, K.W. Cheng, C.S.K. Mak, W.K. Chan, C.T. Yip, Z.T. Liu, A.B. Djurišić, Layer-by-layer deposition of rhenium-containing hyperbranched polymers and fabrication of photovoltaic cells, Chem. Eur. J. 13 (2007) 328–335.
[24] C.M. Halliwell, A.E.G. Cass, A factorial analysis of silanization conditions for the immobilization of oligonucleotides on glass surfaces, Anal. Chem. 73 (2001) 2476–2483.
[25] W.H. Southwell, Pyramid-array surface-relief structures producing antireflection index matching on optical surfaces, J. Opt. Soc. Am. A 8 (1991) 549–553.
[26] B.T. Liu, W.D. Yeh, Reflective properties of nanoparticle-arrayed surfaces, Thin Solid Films 518 (2010) 6015–6021.
[27] S.E. Yancey, W. Zhong, J.R. Heflin, A.L. Ritter, The influence of void space on antireflection coatings of silica nanoparticle self-assembled films, J. Appl. Phys. 99 (2006) 034313-1–034313-10.
[28] A. Deák, I. Székely, E. Kálmán, Zs. Keresztes, A.L. Kovács, Z. Hórvölgyi, Nanostructured silica Langmuir–Boldgett films with antireflective properties prepared on glass substrates, Thin Solid Films 484 (2005) 310–317.
[29] A. Deák, I. Székely, B. Bancsi, A.L. Tóth, A.L. Kovács, Z. Hórvölgyi, Complex Langmuir–Blodgett films from silica nanoparticles: an optical spectroscopy study, Colloid Surf. A—Physicochem. Eng. Aspects 278 (2006) 10–16.
[30] J. Zhu, C.M. Hsu, Z. Yu, S. Fan, Y. Cui, Nanodome solar cells with efficient light management and self-cleaning, Nano Lett. 10 (2010) 1979–1984.
[31] P. Yu, C.H. Chang, C.H. Chiu, C.S. Yang, I.C. Yu, H.C. Kuo, S.H. Hsu, Y.C. Chang, Efficiency enhancement of GaAs photovoltaics employing antireflective indium tin oxide nanocolumns, Adv. Mater. 21 (2009) 1618–1621.